Supplementary Information for:

Fabrication of graphene quantum dot-decorated graphene sheets *via* chemical surface modification

Jaehoon Ryu, Eunwoo Lee, Seungae Lee, and Jyongsik Jang*

School of Chemical and Biological Engineering, College of Engineering, Seoul National University (SNU), Seoul 151-742, Korea.

[*] E-mail: jsjang@plaza.snu.ac.kr
Tel.: +82-2-880-7069
Fax: +82-2-888-1604

1. Experimental Section

***Materials*:** Carbon nanofiber (NEXCARB-H,) was provided by Suntel Co. and used without further purification. Graphite flakes (< 20 μm, synthetic) and 1,5-Diaminonapthalene (DAN) were purchased from Aldrich Chemical Co. and used as received.

***Fabrication of the GQDs*:** The detailed process for preparation of GQDs is presented in our previous paper.[1] The synthesis of the GQDs was based on the oxidation of herringbone carbon nanofibers (H–CNFs). In detail, H-CNFs (30 mg) were mixed with 95 % H_2SO_4 (60 mL) and 60 % HNO_3 (20 mL). The mixture was sonicated for 2 h and then stirred for 24 h at 80 °C. The solution was cooled and diluted with deionized (DI) water (800 mL). NaOH was slowly added to adjust the pH to 8. The GQDs were isolated by size-selective precipitation as follows. The crude solution of GQDs was concentrated to approximately one-fifth of the initial volume. Then, a non-solvent (ethanol) was injected into the concentrated solution until a precipitate formed that consisted of the Na_2SO_4 salts and large-sized graphenes. The resulting turbid solution was separated by centrifugation into a precipitate and supernatant. Ethanol was added to the supernatant, and then it was centrifuged to obtain another supernatant fraction. This process was repeated several more times to produce fraction of GQDs with a uniform size.

***Fabrication of graphene oxide (GO) solution*:** GO powder was prepared by the Hummers method, as presented in our previous paper.[2] A GO solution having a concentration of 5 mg mL^{-1} was obtained by mixing the GO powder with DI water.

***Fabrication of GQDs-decorated graphene sheets*:** The PET substrates were plasma-treated (200 W, 8 SCCM O_2) to modify their surface wettability. The GO aqueous solution (5 mg mL^{-1}) was then coated onto the substrate by spin-coating at 2000 rpm for 30 s. This process was repeated twice more to provide a few layers of GO on the substrate, and then the samples were dried at room temperature. The GO films were then modified by drop-casting a methanolic DAN solution (2, 6, or 20 μM) onto a GO-coated PET substrate over 15 min at room temperature, followed by rinsing with methanol. The GQDs were subsequently drop-cast onto the modified GO surface over 1 h at 100 °C. Finally, the films were reduced by pressure-assisted reduction, which was performed inside a glove box. The sample was placed in a hot press between stainless-steel plates at 180°C for 1 h. The reduction process caused the composite films to change color from brown to metallic gray. The composite was easily transferred by immersion in DI water.

***Photocatalytic activity measurement*:** The photocatalytic performance of the GDGS was measured in terms of the photodegradation of an MB solution under visible-light irradiation. For the measurement, the quantities of the samples were adjusted to equal the intensity of absorbance at 400 nm for comparing the quantum yield during photocatalytic process and summarized in Table S4. The given weight of the as-prepared samples was mixed with 50 mL of an aqueous solution of MB (50 mg L^{-1}). The prepared solution was stirred for 30 min in the dark to achieve adsorption-desorption equilibrium before visible-light irradiation. A xenon lamp (300 W) with a UV cut-off filter ($\lambda > 400$ nm) was used for the photocatalytic test. After every 10 min of irradiation, 4 mL of the photoreacted solution were centrifuged at 12000 rpm for 15 min to remove photocatalysts in the solution. The clear liquid was transferred to a quartz cell (10 mm × 10 mm) for measurement of its absorbance at $\lambda = 660$ nm. The C/C_0 ratio was calculated from these data.

***Characterization*:** TEM and HR-TEM were obtained from JEOL JEM-200CX and JEOL JEM-2010F microscopes, respectively, which are installed at the National Center for Inter-university Research Facilities(NCIRF) at Seoul National University. FTIR spectra were obtained by using Bomem MB100 spectrometer. High-powered XRD (M18XHF-SRA, Mac Science Co., Japan; $\lambda = 1.5406$ Å) and high-resolution Raman microscopy (Horiba Jobin Yvon, France; 514-nm Ar-ion laser) were used to analyze the GQDs, RGO, and GDGS. The surface conductivity of a sample was measured using a Loresta–GP (MCP–T610) resistivity meter (Mitsubishi Chemical Analytech, Japan). XPS spectra were recorded with an AXIS–HIS instrument (KRATOS, United Kingdom). Absorbance and fluorescence emission spectra were acquired using a Lambda–35 UV–Vis spectrophotometer (PerkinElmer, USA) and an FP–6500 spectrofluorometer (JASCO, Japan), respectively.

2. Characterization of as-synthesized GDGS

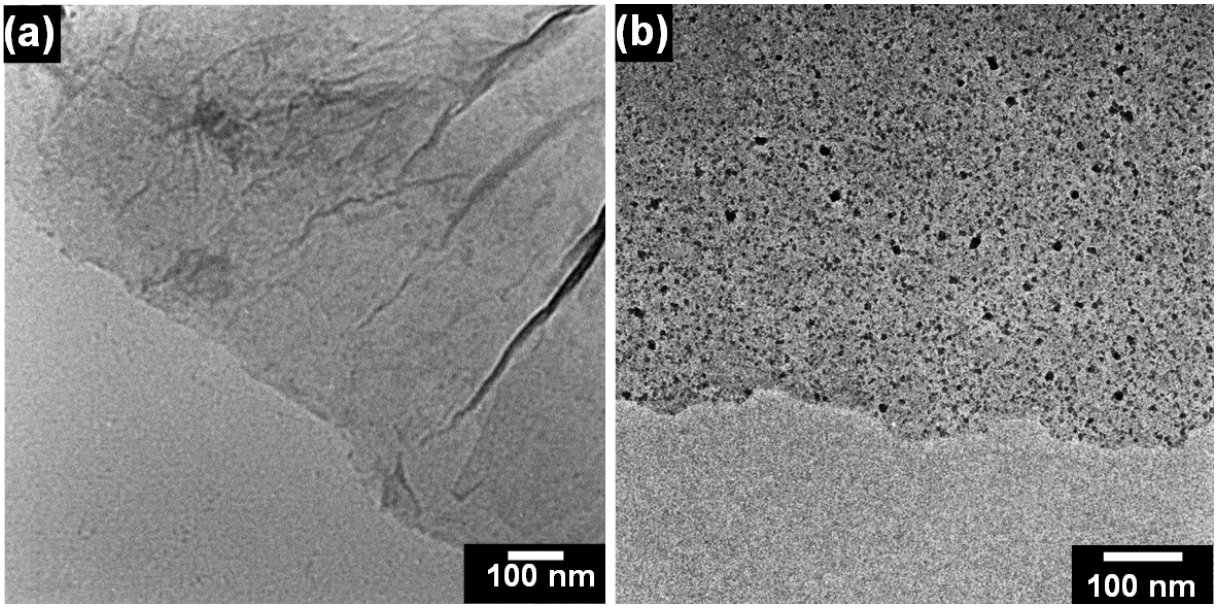

Fig. S1 TEM images for (a) pristine RGO and (b) GDGS–60

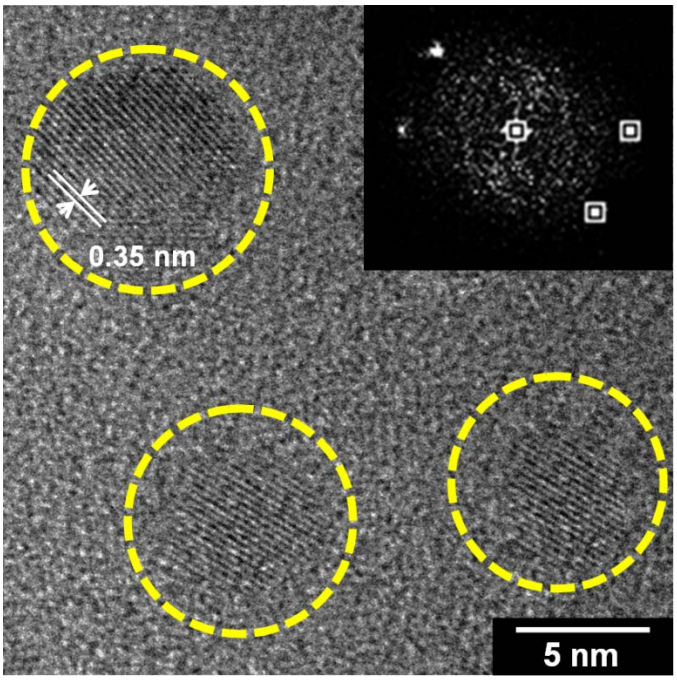

Fig. S2 HR-TEM of GDGS–20 (inset: the corresponding fast Fourier transform pattern).

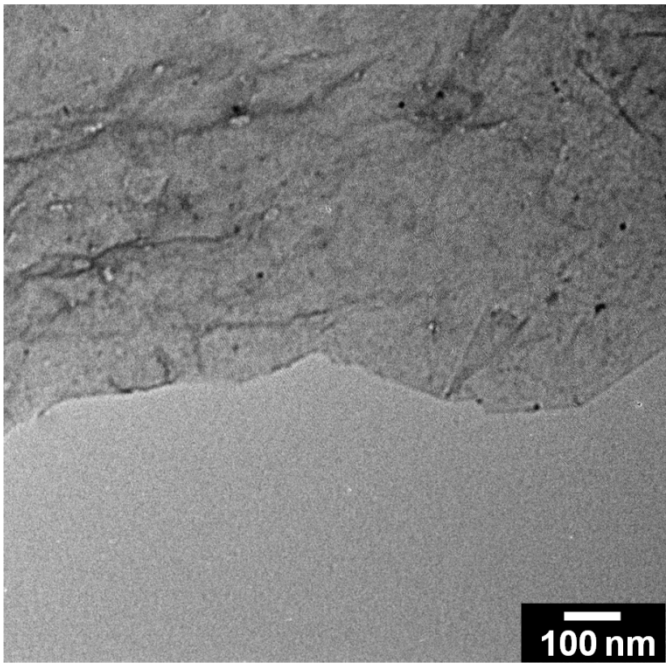

Fig. S3 TEM images of the GDGS which is obtained from the control experiment without DAN.

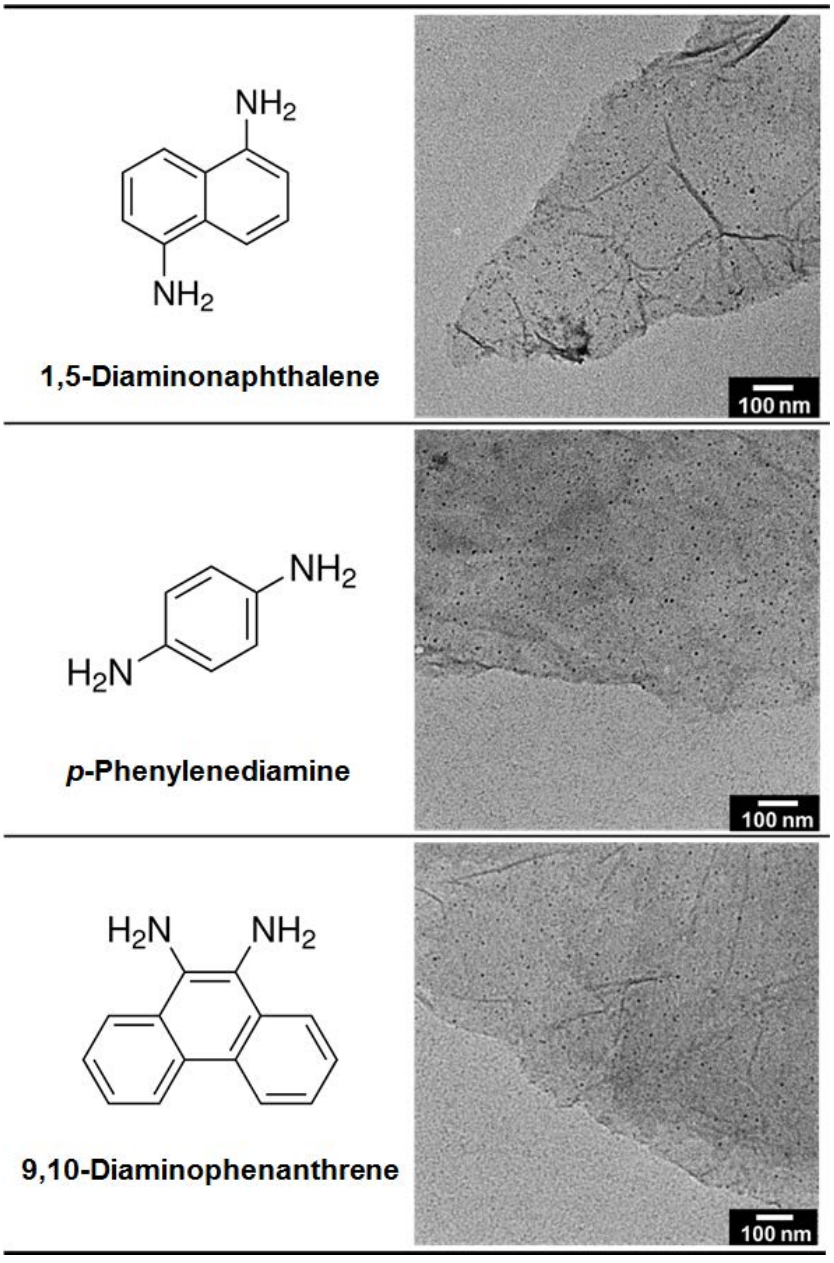

Fig. S4 TEM images of the GDGS with 2 μM of DAN (GDGS-2), and the GDGS prepared under the same conditions except that the DAN was replaced with other aromatic diamino materials as shown in the left column.

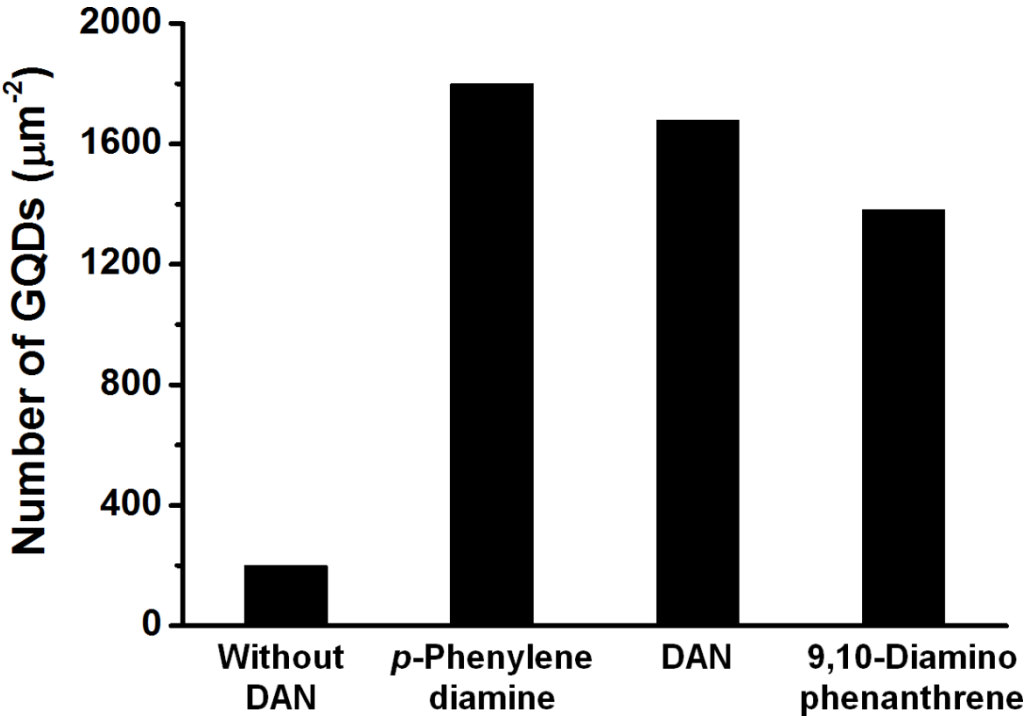

Fig. S5 Variation of the average number of GQDs per unit area of graphene depending on the type of aromatic diamino materials as shown in X axis.

Fig. S3 demonstrates TEM images of the GDGS which is obtained from the control experiment without DAN. GQDs can directly adsorb onto the graphene oxide but, there are few GQDs onto the graphene. This data indicates that the number of sp^2-carbon planes of the GO available for π–π interactions with GQDs were limited due to the functional groups, such as hydroxyl and carboxylic acid groups.

Fig. S4 demonstrates TEM images of the GDGS with 2 μM of DAN (GDGS-2), and the GDGS prepared under the same conditions except that the DAN was replaced with p-phenylenediamine and 9,10-diaminophenanthrene, which are other aromatic diamino materials. All GDGS using three materials shows similar population of GQDs onto graphene and these are summarized in Fig. S5. The population of GQDs was the highest for p-phenylenediamine, followed by diaminonaphthalene and 9, 10-diaminophenanthrene, but there is not a great deal of difference. The differences of GQDs population are attributed to the difference of the number of benzene rings in linker materials to modify the surface of graphene oxide. p-Phenylenediamine can combine more GQDs with graphene compared to the same molar concentration of DAN. However, p-phenylenediamine, which is highly toxic material, is improper to apply in photocatalyst. Moreover, 9,10-diaminophenanthrene is expensive material, thus DAN is among the most advantageous material in the environmental and engineering aspect.

Table S1. Identification of relevant functionalities with the observed significant IR absorption modes.

Components	Assignment	Wavelength (cm^{-1})
GQD	O–H and N–H stretch	3450
	C=O stretch in un-conjugated ketone and carboxyl group	1790
	C=C stretch and secondary amides	1650
	Carboxylic acids and secondary amides	1340
GO	O–H and N–H stretch	3350
	C=O stretch in un-conjugated ketone and carboxyl group	1730
	C=C stretch and secondary amides	1650
	Carboxylic acids and secondary amides	1340
	C–O–C stretch	1040
GDGS	O–H and N–H stretch	3350
	C=O stretch in un-conjugated ketone and carboxyl group	1730
	C=C stretch and secondary amides[a]	1650
	carboxylic acids and secondary amides[b]	1350
	C–O–C stretch	1040
	N–H wag (primary and secondary amides only)[c]	730

[a] The peak is termed the amide I band.

[b] The peak is referred as the amide III band.

[c] The peak is ascribed to N–H wag.

Table S2. Summary of atomic ratio of element to carbon content

Sample	Atomic ratio of element to carbon contents[a]	
	C/O[b]	N/C[c]
GO	1.15	0.034
GQD	2.01	0.038
RGO	1.63	0.028
GDGS–2	1.69	0.031
GDGS–6	1.74	0.035
GDGS–20	1.88	0.044

[a] The ratio of relative area; The area was calculated by integration from corresponding region in XPS spectra.

[b] This value means content ratio of oxygen to carbon; The value is carbon content divided by oxygen content.

[c] This value means content ratio of nitrogen to carbon; The value is nitrogen content divided by carbon content.

Table S3. C1s XPS of surface chemical compositions of GO, RGO, GQD, GDGS-2, GDGS-6, GDGS-20.

Sample	C1s XPS of surface chemical composition (At %)[a]		
	C–C / C=C[b]	C–O / C–N[c]	C=O[d]
GO	59.4	32.1	8.5
RGO	72.9	19.1	8.0
GQD	93.2	2.20	4.6
GDGS–2	73.3	19.0	7.7
GDGS–6	75.3	17.2	7.5
GDGS–20	81.1	14.1	4.8

[a] The ratio of relative area; The area was calculated by integration from corresponding region in C1s XPS spectra. Binding energy is corresponding to [b] 284.5, [c] 286.14 - 286.58, [d] 287.89 – 288.45 eV.

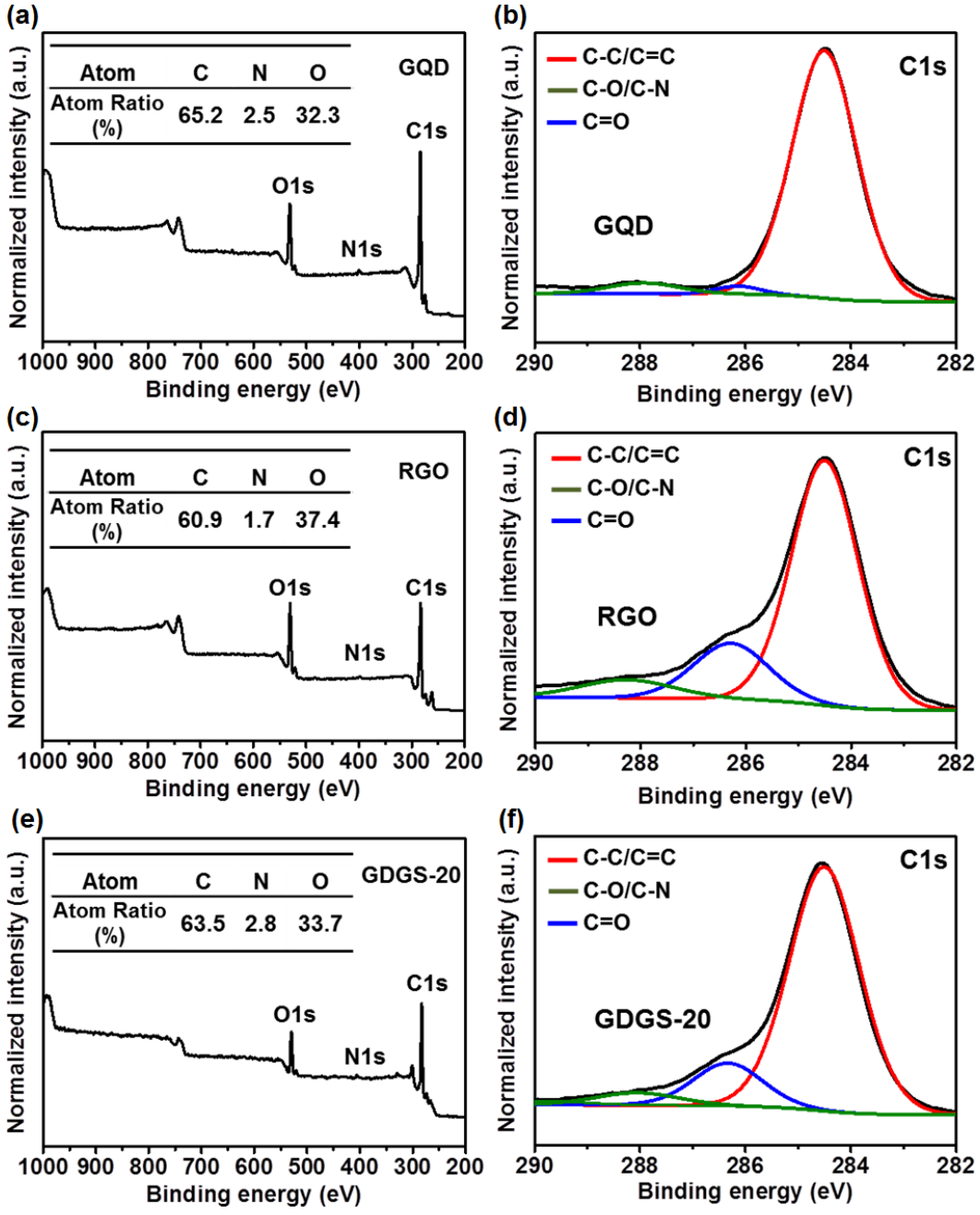

Fig. S6 XPS data of (a) GQD, (c) RGO, and (e) GDGS–20. The insets show the elemental analyses of (a) GQD, (c) RGO, and (e) GDGS–20; C1s XPS spectra of (b) GQD, (d) RGO, (f) GDGS–20.

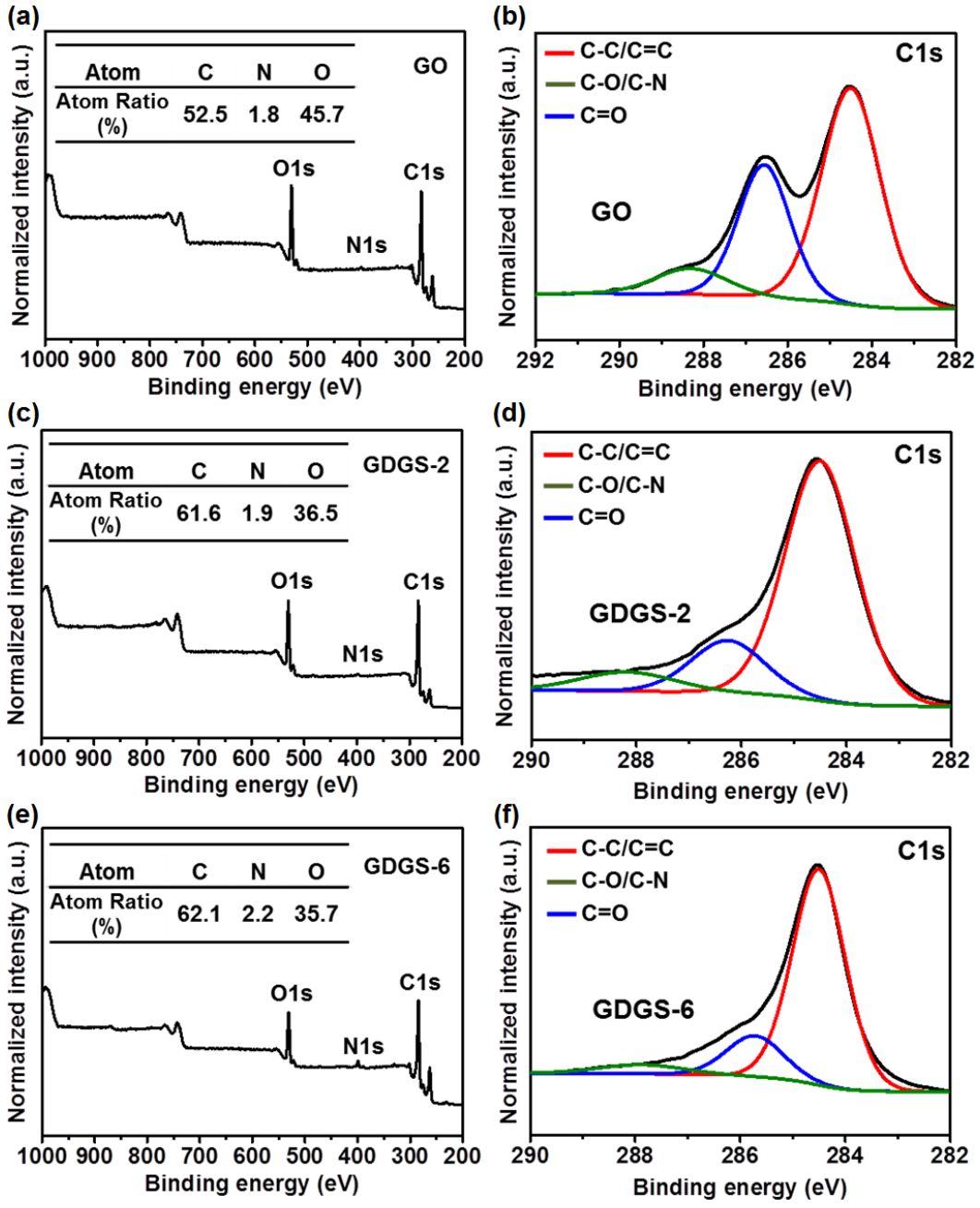

Fig. S7 XPS data of (a) GO, (c) GDGS–2 and (e) GDGS–6. The insets show the elemental analyses of (a) GO, (c) GDGS–2 and (e) GDGS–6; C1s XPS spectra of (b) GO, (d) GDGS–2 and (f) GDGS–6.

XPS was used to quantitatively determine the elemental composition and chemical bonding states of the GDGS. Fig. S3a shows the XPS spectra of the GQDs over the range of 200–1000 eV. The GQDs were composed of carbon (65.2%), oxygen (32.3%), and nitrogen atoms (2.5%) (inset of Fig. S3a). The GQDs had the highest C/O ratio (Table S2). The C, N, and O contents of the RGO and the GDGS–20 are shown in the inset of Fig. S3c and e, respectively. A higher C content and a lower O content were observed for GDGS than for RGO. This result indicates that large numbers of GQDs, which have the highest C/O ratio, were combined with RGO and the GDGS C/O ratio is a measure of the GQD population on the graphene sheets. Additionally, the higher N content was attributed to the use of DAN, which subsequently led to formation of amide bonds. The changing GQD population was further explored by analyzing the XPS spectra of the GDGS–x (x = 2, 6) (Fig. S4). The C/O ratio was the highest for GDGS–20, followed by GDGS–6 and GDGS–2. This indicated that the GQD population on the graphene sheets increased with increasing concentration of the DAN solution. The XPS C1s spectra also confirmed these population changes. . Fig. S3b, d, and f show the XPS C1s spectra of the GQDs, RGO, and GDGS–20, respectively; the C–C/C=C, C–O/C–N, and C=O chemical composition ratios are summarized in Table S3. The graphitic sp^2-carbon (C–C/C=C) ratio was higher in the GDGS–20 than in the RGO. This was ascribed to the decoration of great numbers of GQDs on the RGO surface. The GDGS C–C/C=C ratio increased with increasing number of decorating GQDs because of the higher graphitic sp^2-carbon ratio for the GQDs (93.2%) compared with RGO (72.9%). It is reasonable to use the C–C/C=C ratio for GDGS as an indicator of the extent of the GQD population of GDGS. The graphitic sp^2-carbon ratio was the highest for the GDGS–20, followed by the GDGS–6 and GDGS–2. Consequently, the GDGS–20 contained the highest population of decorating GQDs, followed by GDGS–6 and GDGS–2.

Although the number of DAN modified onto the graphene is increasing, the number of N in DAN is relatively very low compared to the number of C in graphene, and the number of GQD bonded onto the graphene also increases. Due to these reasons, the ratio of N to all atoms (C, N, O) in GDGS-x (x=2-60) is close. However, the concentration of N in GDGS-x (x=2-60), even if the values are very small, showed a tendency to increase with increasing the concentration of DAN. This tendency indicates the increase of DAN modified onto the graphene. Though the concentration of both N and C increased due to the increase of GQD and DAN, the increase rate of N from DAN is relatively high compared to the increase rate of C from GQD due to the existence of a large quantity of C in graphene sheet. This tendency can also easily be verified by value of N/C value in Table S2.

4. Pressure-assisted reduction method

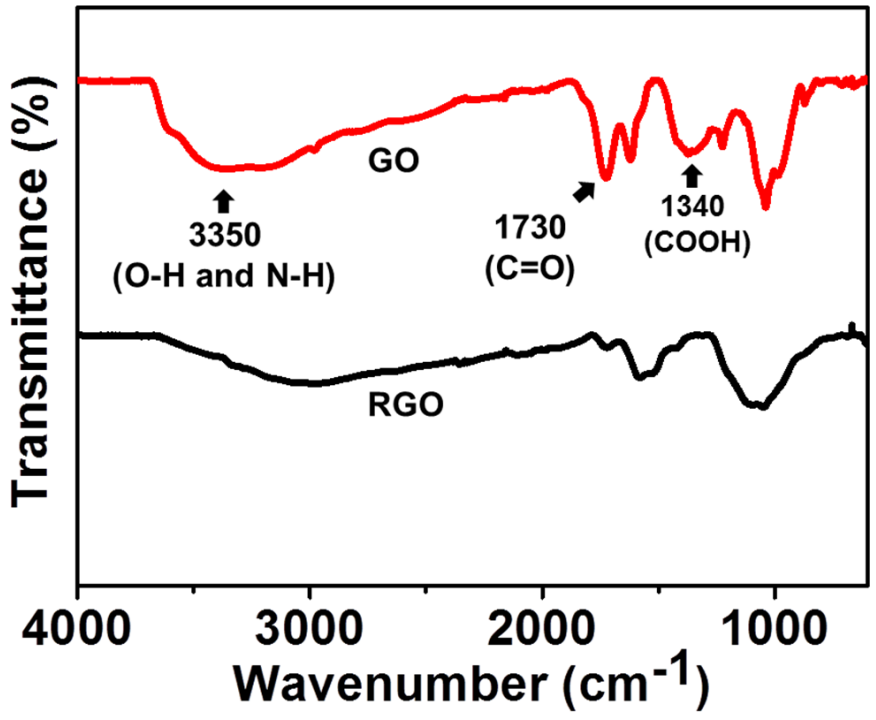

Fig. S8 FTIR spectra of GO and RGO.

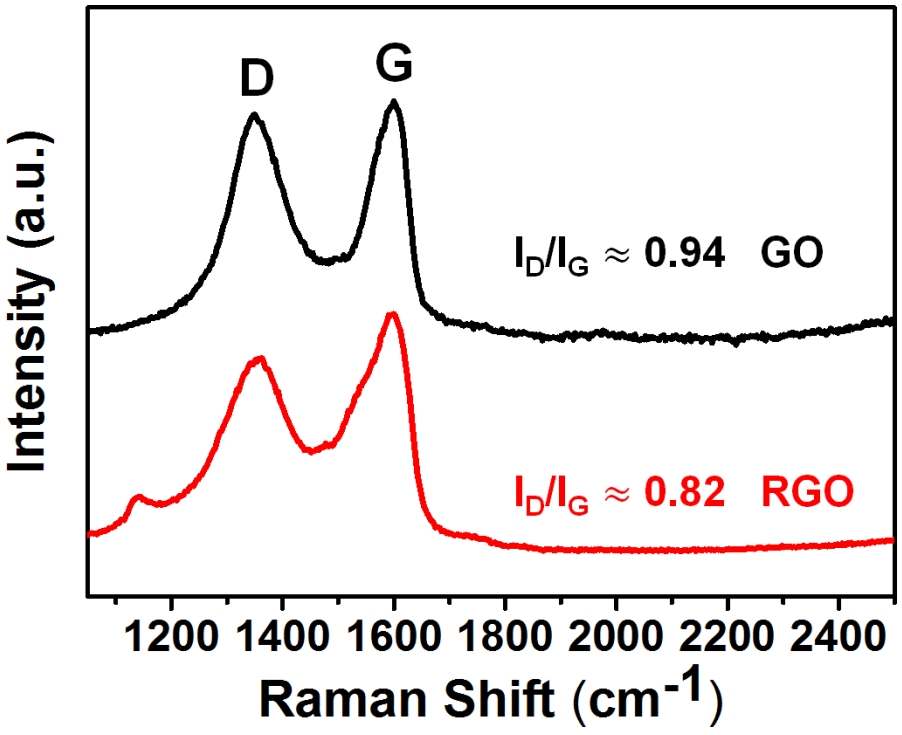

Fig. S9 Raman spectra of GO and RGO.

New peak appeared at 1130 cm^{-1} in the RGO, which originates from carbon-carbon stretching modes of alkyl groups.[3]

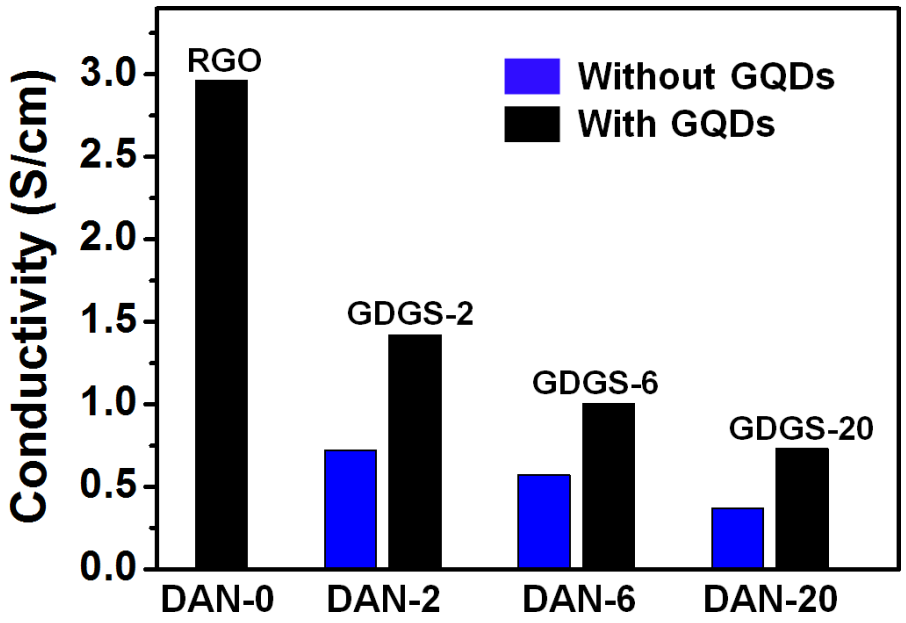

Fig. S10 Conductivity of RGO, GDGS-x (x=2, 6, 20) and modified-RGO as a function of molar concentration of DAN (2, 6, 20 μM).

5. Photocatalytic degradation process

The separated electrons react with O_2 to yield superoxide radical anions $O_2^-\bullet$ in aerated conditions, and the holes generate "•OH" from absorbed H_2O molecules or directly oxidize the organic pollutants as following equation.[4]

$$O_2 + e^- \rightarrow O_2^-\bullet \quad \textbf{(1)}$$

$$H_2O + h^+ \rightarrow \bullet OH + H^+ \quad \textbf{(2)}$$

$$R\text{—}H + h^+ \rightarrow RH^+\bullet \rightleftharpoons R\bullet + H^+ \quad \textbf{(3)}$$

The produced radicals degraded organic pollutants through subsequent radical reactions as following equation.

$$R\text{—}H + \bullet OH \rightarrow R\bullet + H_2O \quad \textbf{(4)}$$

$$R\bullet + O_2 \rightarrow ROO\bullet \xrightarrow{O_2/H_2O} \text{Degradation} \quad \textbf{(5)}$$

$$R\text{—}H + \bullet OH \rightarrow HROH\bullet \xrightarrow{O_2/H_2O} \text{Degradation} \quad \textbf{(6)}$$

6. Photoactivity and durability test of GDGS

Table S4. Summary of weight of the used samples for photoactivity test

Sample	Weight (mg)[a]
GQD	88.76
GDGS-20	50
GDGS-6	44.38
GDGS-2	37.38
RGO	33.86

[a] The adjusted weight of each sample to equal the intensity of absorbance at 400 nm

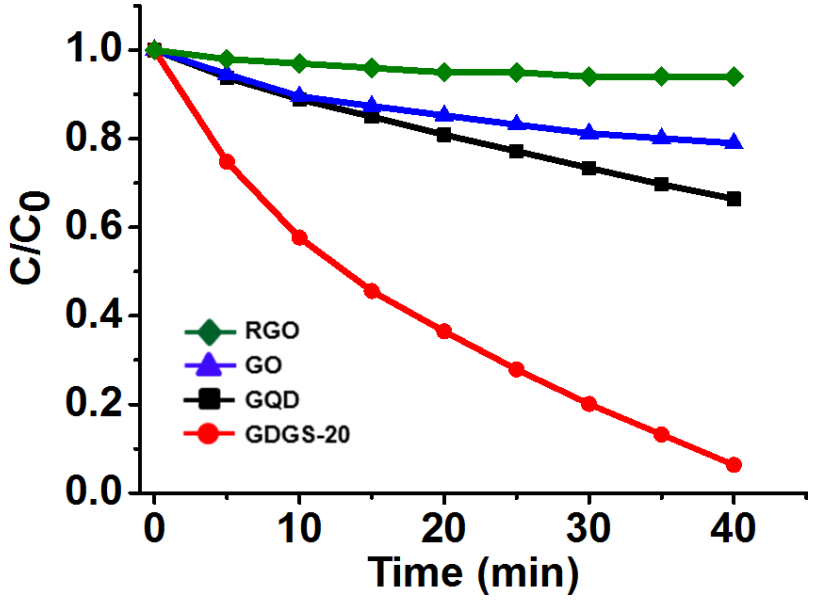

Fig. S11 Photocatalytic degradation of MB over the GO, RGO, GQDs and GDGS–20; 50 mg of samples were mixed with 50 mL of an aqueous solution of MB (50 mg L^{-1})

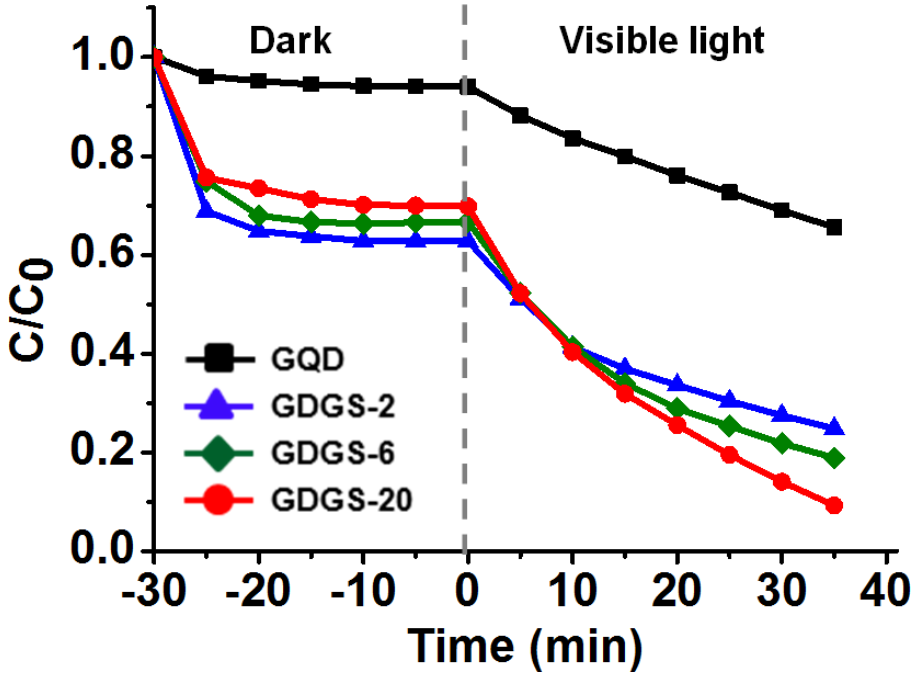

Fig. S12 Photocatalytic degradation of MB over the GQDs and GDGS–x (x = 2, 6, 20); 50 mg of samples were mixed with 50 mL of an aqueous solution of MB (50 mg L^{-1})

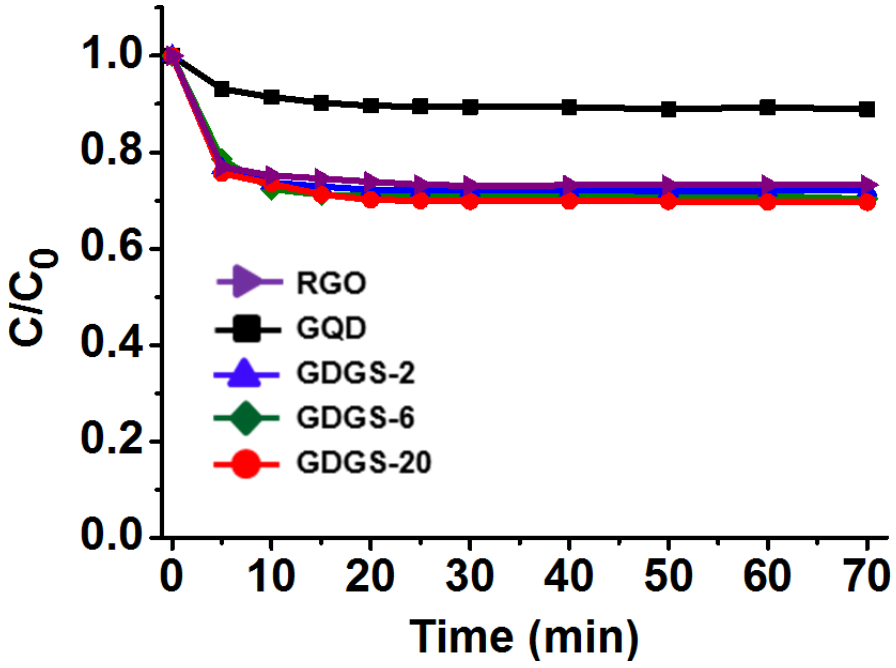

Fig. S13 Photocatalytic degradation of MB over the RGO, GQDs and GDGS–x (x = 2, 6, 20) in dark condition

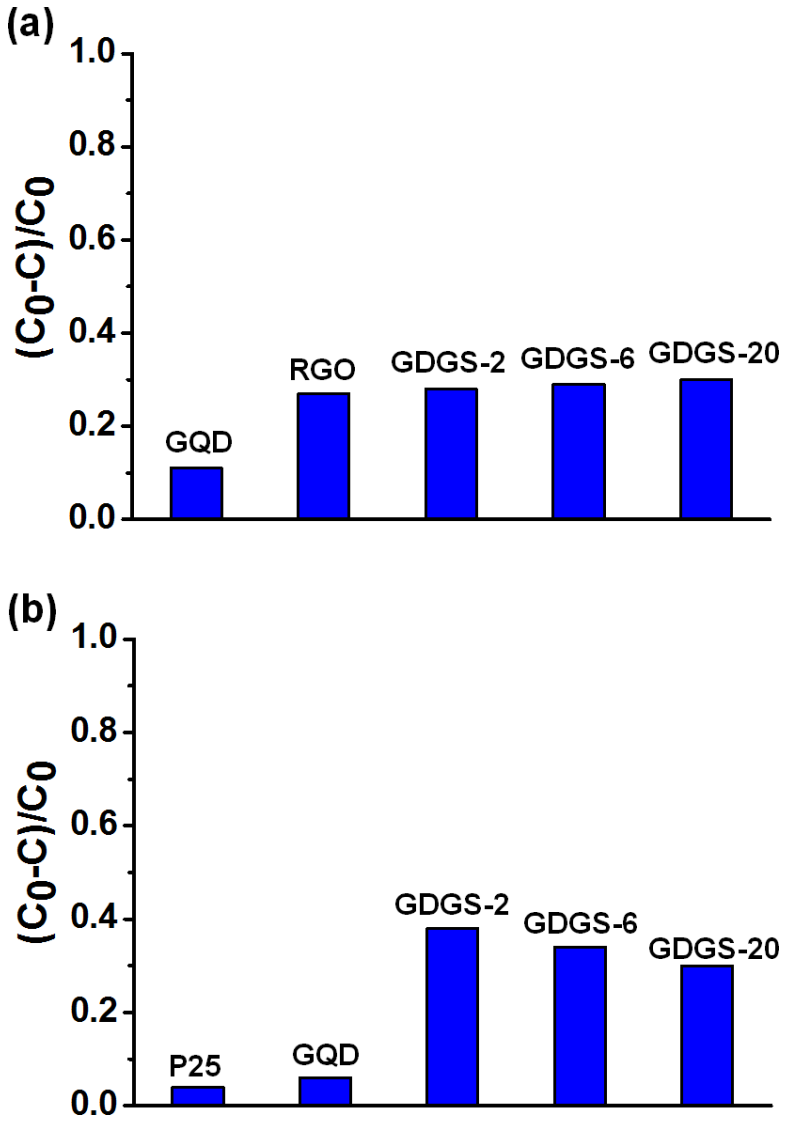

Fig. S14 Adsorption capacities of MB in the dark for 30 min on different samples; corresponding experiments performed with samples at (a) constant absorbance at 400 nm and with (b) constant weight (50 mg) of the samples

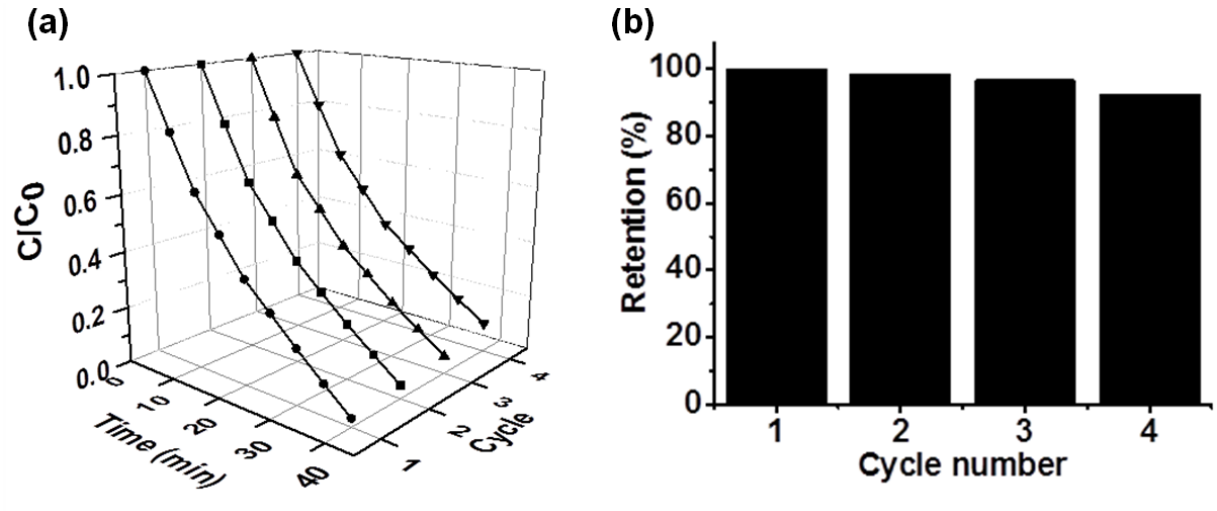

Fig. S15 (a) Photo-degradation curves for four consecutive cycles and (b) Cycling performance of GDGS-20.

Photodegradation test of MB repeated four times to verify the durability of as-prepared GDGS. The test was carried out with GDGS-20, which exhibited the best photocatalytic efficiency under experimental condition. Photocatalysts were recovered by centrifugation after degradation of dye and then, new MB solution was added. Retention in Fig. S5 stands for the ratio of degraded MB amount at each cycle to that at first cycle. Significant change of decompose curve were not observed and the retention value after 4 cycles showed 92.5 %, indicating that GDGS also has high stability.

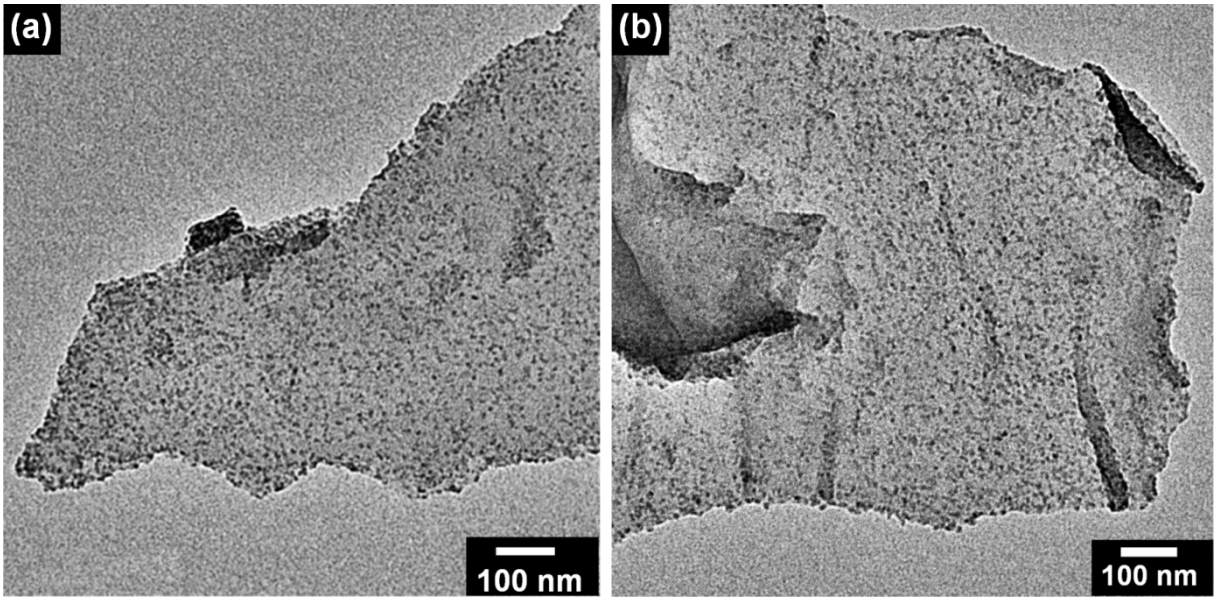

Fig. S16 TEM image of GDGS-20 (a) before and (b) after visible light irradiation during 1h.

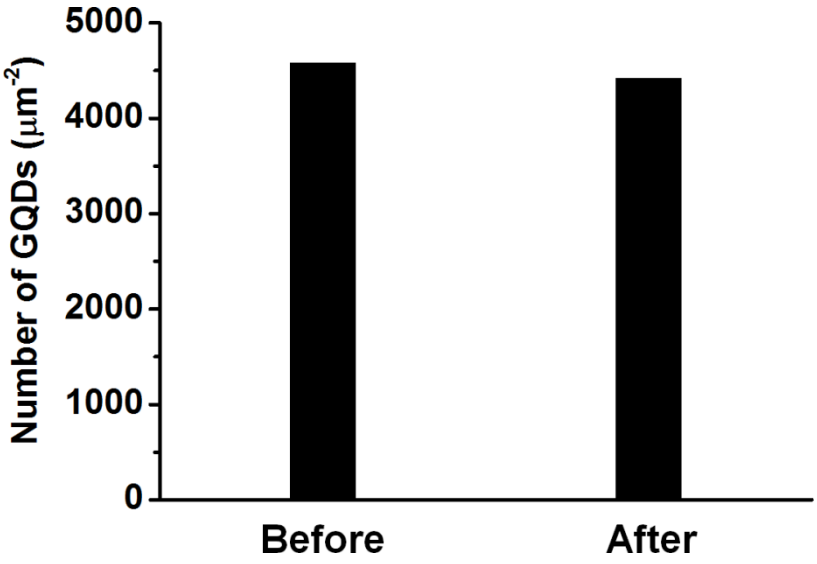

Fig. S17 The average number of GQDs per unit area in GDGS-20 before and after visible light irradiation.

7. Photocatalysis mechanism of GDGS

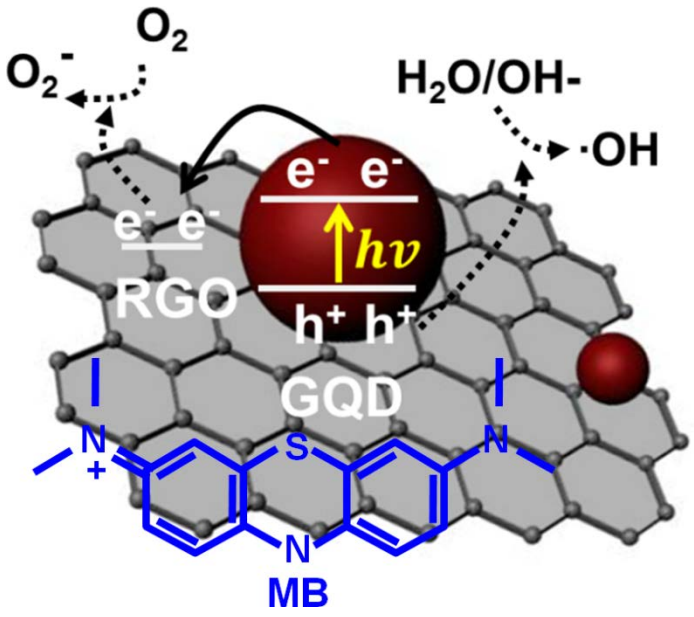

Fig. S18 Scheme of the proposed photocatalytic mechanism of the GDGS

8. References

1. E. Lee, J. Ryu and J. Jang, *Chem. Commun.*, 2013, **49**, 9995-9997.
2. S. Lee, C.-M. Yoon, J.-Y. Hong and J. Jang, *Journal of Materials Chemistry C*, 2014.
3. B. Zhang, L. Li, Z. Wang, S. Xie, Y. Zhang, Y. Shen, M. Yu, B. Deng, Q. Huang, C. Fan and J. Li, *J. Mater. Chem.*, 2012, **22**, 7775-7781.
4. C. Chen, W. Ma and J. Zhao, *Chem. Soc. Rev.*, 2010, **39**, 4206-4219.